A&A 533, A117 (2011)
DOI: 10.1051/0004-6361/201116644

Astronomy & Astrophysics

On the missing 2175 Å-bump in the Calzetti extinction curve

J. Fischera[1] and M. Dopita[1,2]

[1] Research School of Astronomy & Astrophysics, Mount Stromlo Observatory, Cotter Road, Weston Creek, ACT 2611, Australia
e-mail: fischera@mso.anu.edu.au
[2] Astronomy Department, Faculty of Science, King Abdulaziz University, PO Box 80203, Jeddah, Saudi Arabia

Received 4 February 2011 / Accepted 13 July 2011

ABSTRACT

Aims. The aim of the paper is to give a physical explanation of the absence of the feature in the Calzetti extinction curve.
Methods. We analyze the dust attenuation of a homogeneous source seen through a distant inhomogeneous distant screen. The inhomogeneities are described through an idealized isothermal turbulent medium where the probability distribution function (PDF) of the column density is log-normal. In addition it is assumed that below a certain critical column density the carriers of the extinction bump at 2175 Å are being destroyed by the ambient UV radiation field.
Results. Turbulence is found to be a natural explanation not only of the flatter curvature of the Calzetti extinction curve but also of the missing bump provided the critical column density is $N_{\rm H} \geq 10^{21}$ cm^{-2}. The density contrast needed to explain both characteristics is well consistent with the Mach number of the cold neutral medium of our own Galaxy which suggests a density contrast $\sigma_{\rho/\langle\rho\rangle} \approx 6$.

Key words. turbulence – dust, extinction – ISM: structure

1. Introduction

The ability of interstellar dust grains to attenuate light through scattering and absorption can lead to large uncertainties in the determination of the crucial physical parameters of galaxies. These parameters not only help determine the evolution of the galactic system, but are also important for the determination of the star formation rate as function of red-shift, a key parameter in understanding the evolution of the universe as a whole. The dust correction is complicated by several effects as the contribution of scattered light, the geometry, the mixture of the dust with the sources, and the inhomogeneous structure of the interstellar medium all affect the global attenuation of the galactic starlight. These effects produce an attenuation curve which may be quite different from a pure extinction curve derived for an individual star.

It is maybe not too surprising that the galactic reddening curve $E(\lambda - V)/E(B - V)$ derived for star-burst galaxies (Calzetti 2001) shows two significant deviations from the extinction curve known for the diffuse interstellar medium (ISM) of our own galaxy. First the reddening at long wavelengths is lower which points to a larger absolute-to-relative extinction R_V and to flatter extinction curve A_λ/A_V and second the 2175 Å feature which is very prominent in the extinction curves derived for the Milky Way or the Large Magellanic Cloud (LMC) seems to be rather weak or absent. The smoothness makes the Calzetti curve similar to the extinction curve derived for the bar of the Small Magellanic Cloud (SMC) (Gordon & Clayton 1998). However, the overall curvature in the optical is steeper in the SMC with an R_V-value even slightly lower (2.74 ± 0.13, Gordon et al. 2003) in respect to the Milky Way (3.1, Fitzpatrick 1999).

A flatter curvature of a pure foreground extinction points in general to a larger grain population as is inferred in the case of the Orion region, for example. A flattening of the effective extinction curve for extended sources can also be produced by the in-homogeneity of the dusty interstellar medium. The reason for this lies in the fact that a non-homogeneous medium is less optically thick than a homogeneous distribution of matter and that the reduction in the effective extinction increases with optical thickness. It has been found based on radiative transfer calculations that a clumpy shell can reproduce the Calzetti curve if dust properties are consistent with the smooth SMC bulk extinction curve (Gordon et al. 1997; Witt & Gordon 2000). We have shown (Fischera et al. 2003) that the overall flatter curvature of the Calzetti curve can be naturally explained by the turbulent nature of the ISM (Paper I). The density contrast needed to produce the flattening is found to be consistent with the velocity dispersion of the cold neutral medium (CNM) as indicated by CO observations.

The situation with regard to the absence of the peak at 2175 Å is rather different. It is thought that the peak is caused by π-electron resonance produced in small carbonaceous particles which include graphenes, polycyclic aromatic hydrocarbons (PAH) and possibly small graphite grains (Li & Draine 2001; Weingartner & Draine 2001; Draine & Li 2007; Fischera & Dopita 2008). The UV light is thought to excite the skeleton vibration modes of the molecules which produce in case of PAH molecules the broad emission features seen in the near infrared. The analysis of the diffuse galactic emission (Witt & Lillie 1973; Lillie & Witt 1976; Morgan et al. 1976) or reflection nebula (Witt et al. 1982, 1992; Calzetti et al. 1995) suggests that the feature is predominantly or even completely caused by absorption. If the observed light contains a considerable amount of scattered emission the peak strength in the effective extinction curve would even increase. Simple geometrical effects are therefore an unlikely explanation for the absence of the feature in the Calzetti curve as verified by detailed radiative transfer calculations (Gordon et al. 1997; Witt & Gordon 2000). On the other hand it has been argued that the Calzetti curve is a result of an additional clumpy distribution of the stars where young

stars are strongly mixed with opaque clouds (Granato et al. 2000; Panuzzo et al. 2007).

A possible origin for the smooth Calzetti curve lies in the destruction of the carriers of the peak caused by the strong UV radiation field. This process has been discussed in the context of star burst galaxies by Dopita et al. (2005), and has been extensively modeled by several authors (Omont 1986; Allamandola et al. 1989; Léger et al. 1989; Allain et al. 1996a,b; Le Page et al. 2003) A similar interpretation was given for the absence of the peak in the SMC bar extinction curve. The carriers are thought to be destroyed by the pervasive UV radiation field caused by the lower dust content resulting from a ten times (Russell & Dopita 1992) lower metallicity in the ISM of the SMC (Gordon & Clayton 1998). The destruction in the ISM cannot be complete as one individual sight line shows a clear extinction bump (Lequeux et al. 1982; Gordon & Clayton 1998; Gordon et al. 2003). A complete destruction of the carriers also seems to be in contradiction with the observed emission spectra of starburst galaxies as they still show the prominent PAH emission features.

This paper is number IV in a series of papers where we analyze the attenuation characteristics caused by a dusty turbulent medium. In the first paper (Paper I) we addressed the problem if a turbulent medium can reproduce the flatter curvature of the Calzetti extinction curve. In the following paper (Fischera & Dopita 2004) we provided a model of the isothermal turbulent screen and showed how the statistical properties (the 1-point and the 2-point statistic) of the column density are related to the statistical properties of the local densities (Paper II). We have applied this model (Fischera & Dopita 2005) to analyze in detail the attenuation caused by a distant turbulent screen (Paper III). In this current paper we investigate under which circumstances the 2175 Å absorption feature can be suppressed, while at the same time not removing all its carriers through PAH photo-dissociation.

2. Model

In any model, the geometry of the dust with respect to an extended source of photons is crucial in determining the received intensity at any wavelength. As in our previous Paper III we will apply the geometry of a distant turbulent dusty screen.

2.1. The turbulent slab

For the dusty screen we assume an isothermal turbulent medium. Turbulence produces a broad distribution of the local density ρ which is because of the dependence of the densities from their neighboring density values described in the absence of gravity through a log-normal function. If we consider the normalized values $\hat{x} = x/\langle x\rangle$ where $\langle x\rangle$ is the mean the probability distribution function (PDF) is given by:

$$p(\ln\hat{x}) = \frac{1}{\sqrt{2\pi}\sigma_{\ln\hat{x}}}\exp\left[-\frac{1}{2\sigma^2_{\ln\hat{x}}}\left(\ln\hat{x}-\ln\hat{x}_0\right)^2\right] \quad (1)$$

with $\ln\hat{x}_0 = -\frac{1}{2}\sigma^2_{\ln\hat{x}}$ where $\sigma_{\ln\hat{\rho}}$ is the standard deviation of the log-normal function. The standard deviation of the log-normal function is directly related to the standard deviation of the normalized values:

$$\sigma_{\hat{x}} = \sqrt{\mathrm{e}^{\sigma^2_{\ln\hat{x}}}-1} \quad (2)$$

In case of the local density the density contrast is according to Padoan et al. (1997) directly related to the Mach number $\delta v/cM$ (where δv is the velocity dispersion and c the sound speed) in the medium with $\sigma_{\hat{\rho}} = \beta M$ with $\beta = 1/2$. For the cold neutral medium (CNM) in our galaxy the CO measurements for example imply a Mach number $M \approx 12$ which provides $\sigma_{\hat{\rho}} \approx 6$.

The log-normal function is very robust and becomes only skewed in in the presence of self-gravity. This produces higher probabilities of encountering high densities since those values are located in the massive clouds which are gravitationally more stable against the turbulent motion.

The log-normal function Eq. (1) also approximately applies to the distribution of the normalized column density $\xi = N_\mathrm{H}/\langle N_\mathrm{H}\rangle$ through an idealized turbulent medium Fischera et al. (2003). We have shown how the ratio of the standard deviation of the column density and the standard deviation of the local density depends apart from the thickness Δ of the turbulent slab which is conveniently measured in terms of the maximum turbulent scale L_max also on the structure of the local density. In the turbulent medium the structure is described through a simple power law of the local density in Fourier space $P(\rho(k)) = k^n$ where k is the wavenumber. In the limit of a thin slab ($\Delta/L_\mathrm{max} \ll 1$) the standard deviations become equal. In the limit of a thick screen ($\Delta/L_\mathrm{max} \gg 1$) the variance of the column density is inversely proportional to the thickness. Assuming a simple power law this limit is given by:

$$\sigma_\xi = \sigma_{\rho/\langle\rho\rangle}\sqrt{\frac{n+3}{2n+4}\frac{L_\mathrm{max}}{\Delta}}, \quad (3)$$

where $n < -3$. The value $n = -11/3$ is consistent with Kolmgorov turbulence. As shown in Paper II the asymptote also provides accurate results at $\Delta/L_\mathrm{max} = 1$.

In this model the standard deviation of the column density is not clearly defined as the value depends not only on the turbulence of the medium (Mach number M) but also on the thickness of the slab Δ/L_max. The same distribution function can be obtained through different assumptions of the turbulence and the slab thickness. In this work we consider therefore the distribution function of the column density assuming different values of the total mean column density and the standard deviation $\sigma_{\ln\xi}$.

2.2. The effective extinction

We assume that the carriers of the 2175 Å bump are being destroyed below a certain column density $[N_\mathrm{H}]_\mathrm{crit} = \xi_\mathrm{crit}\langle N_\mathrm{N}\rangle$ but intact at higher column densities. The corresponding extinction coefficients in the medium below and above this critical column density are distinguished as $\kappa^{(1)}_\lambda$ and $\kappa^{(2)}_\lambda$, respectively.

The effective or effective extinction of a homogeneous light source seen through a turbulent, or in general non-homogeneous, dusty screen is given by the mean of the extinction values

$$\tau^\mathrm{eff}_\lambda = -\ln\langle\mathrm{e}^{-\tau_\lambda}\rangle \quad (4)$$

where $\tau_\lambda = \kappa_\lambda N_\mathrm{H}$ is the optical depth. For the idealized turbulent screen the effective extinction is then given by:

$$\mathrm{e}^{-\tau^\mathrm{eff}_\lambda} = \int_{-\infty}^{y_\mathrm{crit}} \mathrm{d}y\,\mathrm{e}^{-\langle\tau^{(1)}_\lambda\rangle\mathrm{e}^y}\,p(y) + \mathrm{e}^{-\Delta\langle\tau_\lambda\rangle\mathrm{e}^{y_\mathrm{crit}}}\int_{y_\mathrm{crit}}^{\infty}\mathrm{d}y\,\mathrm{e}^{-\langle\tau^{(2)}_\lambda\rangle\mathrm{e}^y}\,p(y) \quad (5)$$

where $\langle\tau^{(i)}_\lambda\rangle = \kappa^{(i)}_\lambda\langle N_\mathrm{H}\rangle$ is the mean extinction and where we use the abbreviation $y = \ln\xi$ and $y_\mathrm{crit} = \ln\xi_\mathrm{crit}$. Further, we have difference in optical depth $\Delta\langle\tau_\lambda\rangle = \langle\tau^{(1)}_\lambda\rangle - \langle\tau^{(2)}_\lambda\rangle$.

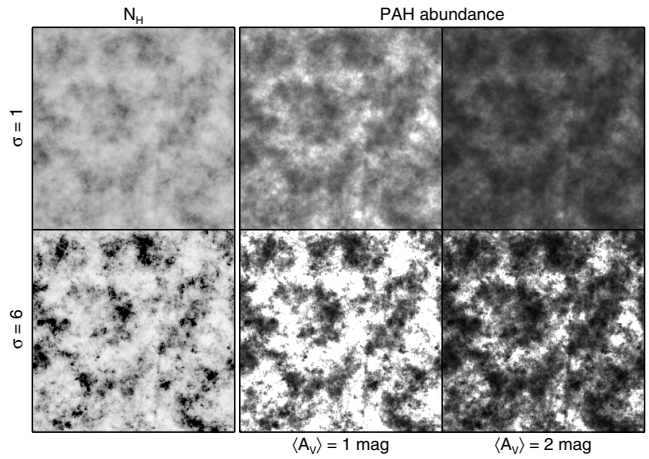

Fig. 1. Visualization of the effect caused by PAH destruction below a critical column density $[N_{\rm H}]_{\rm crit} = 10^{21}$ cm^{-2}. The density structure is derived using a cube of 256^3 Pixel, a power index of $n = -10/3$ and a maximum length scale of 0.4 times the cube size. To the left the column density for two standard deviations $\sigma_{\rho/\langle\rho\rangle}$ of the local density is shown. The images to the right for each turbulent cube gives the PAH abundance along individual sight lines for two assumptions of the extinction A_V through the cube. The white fields correspond to no PAH molecules while the black fields have the normal PAH abundance necessary to produce the extinction bump at 2175 Å.

The effect caused by the destruction of PAH molecules below a column density of $[N_{\rm H}]_{\rm crit} = 10^{21}$ cm^{-2} is visualized in Fig. 1 for two different assumptions of the density contrast and the mean extinction $\langle A_V\rangle$ through the slab. The density contrasts 1 and 6 correspond, assuming a power $n = -10/3$, to a standard deviation $\sigma_{\ln\xi}$ of the log-normal density distribution of the column density of approximately 0.22 and 1.01.

The turbulence produces a large variety of column densities. In high turbulent media the medium is compressed to small volumes of high densities which appear in projection as individual clouds leaving large areas of low column densities. An appreciable fraction of the total projected area is completely free of the carriers of the 2175 Å absorption feature. As more light is transmitted in these regions, the size of the bump in the overall attenuation curve is reduced as well.

On the other hand the carrier abundance of the bump is higher in a turbulent medium as the dust is now found predominantly in dense clouds where the carriers become because of the high column densities save against destruction.

2.3. Extinction curve

For the calculations we adopt the extinction curve as provided by Fitzpatrick (1999). In the model the feature at 2175 Å is described by a Drude model which we subtracted to obtain the curve for a medium where the carriers are destroyed. For simplicity we assume that the absolute-to-relative extinction does not depend on the carrier destruction. To analyze the effect of the destruction on the attenuation curve we consider the extinction coefficients at peak frequency. The corresponding values without and with the absorption feature are given by:

$$\kappa^{(1)}_{0.22} = 5.75/(5.8\times10^{21})\ {\rm cm}^{-2},$$
$$\kappa^{(2)}_{0.22} = 8.78/(5.8\times10^{21})\ {\rm cm}^{-2}. \quad (6)$$

As peak strength we define

$$\frac{\Delta A_{0.22}}{E(B-V)} \quad (7)$$

where $\Delta A_{0.22}$ is the difference of the extinction at peak frequency with and without absorption feature. In case of the Fitzpatrick curve this value is $c_3/\gamma^2 = 3.30$ where $c_3 = 3.23$ is the bump strength and $\gamma = 0.99$ the bump width (Fitzpatrick 1999).

3. Results

First we show that a turbulent medium with the combination of additional destruction can indeed lead to a reduced feature at 2175 Å. We will then analyze more quantitative the requirements to produce smooth attenuation curves. Approximations of the effective optical depths are given in Appendix A.

3.1. The attenuation curve

To derive attenuation curves we assume for the critical column density below which the carriers of the extinction bump are destroyed $[N_{\rm H}]_{\rm crit} = 10^{21}$ cm^{-2}. For the dusty screen we assumed several values of the standard deviation $\sigma_{\ln\xi}$ of the log-normal distribution of the column density spanning a range from a smooth ($\sigma_{\ln\xi} = 0.125$) to a highly non homogeneous medium ($\sigma_{\ln\xi} = 2$). To show the effect on the extinction value we considered two mean values $\langle A_V\rangle = 1$ mag and $\langle A_V\rangle = 2$ mag.

The derived curves are shown in Fig. 2. The important parameters characterizing the curves are summarized in Table 1 which are the effective absolute-to-relative extinction $R^A_V = A^{\rm eff}_V/E(B-V)^{\rm eff}$, the extinction in V-band $A_V/\langle A_V\rangle$, and the peak strength c_3/γ^2 which is analyzed more quantitatively in Sect. 3.2. In addition the table lists the density contrast for certain assumptions for the power n and the thickness of the screen relative to the maximum cloud size. The density contrast for $\sigma_{\ln\xi} = 2$ is already more than two times higher than is implied by CO measurements. In this regard the physical conservative regime is limited to $\sigma_{\ln\xi} < 2$. In systems with higher star formation rates like in star burst galaxies which lead to stronger turbulence the distributions are possibly wider.

As visualized in Fig. 2, the distant screen becomes more transparent for wider distributions of the column densities. This effect is stronger in more optically thick media. In the optical this produces a flatter effective extinction curve which leads to a larger absolute to relative extinction R^A_V. As shown in Table 1 for the considered parameters a broader distribution of the column density produces a flatter extinction curve. However, we note that for extremely broad distributions this behavior is not valid for opaque screens ($\langle A_V\rangle > 1$ mag) as is shown in the next section. As we have shown in our Paper I that the turbulent distant screen model suggests for the Calzetti extinction curve an R^A_V-value larger than 4. Our best solution provides $R^A_V \sim 4.75$. This implies $\sigma_{\ln\xi} > 1$ for both extinction values.

To emphasize the effect of the carrier destruction of the 2175 Å bump we considered also a turbulent medium where the carrier abundance is naturally lower. In case of a smooth medium the two curves become identical. As can be seen in Fig. 2, in case of a naturally lower carrier abundance the peak strength only mildly decreases for broader distributions which keeps to be prominent feature in the effective extinction curve. In contrast, if the abundance changes according to the column density because of destruction the peak weakens strongly for wider column density distributions. For example, for $\sigma_{\ln\xi} > 1$ the peak strength is less than 20% of the intrinsic value (Table 1).

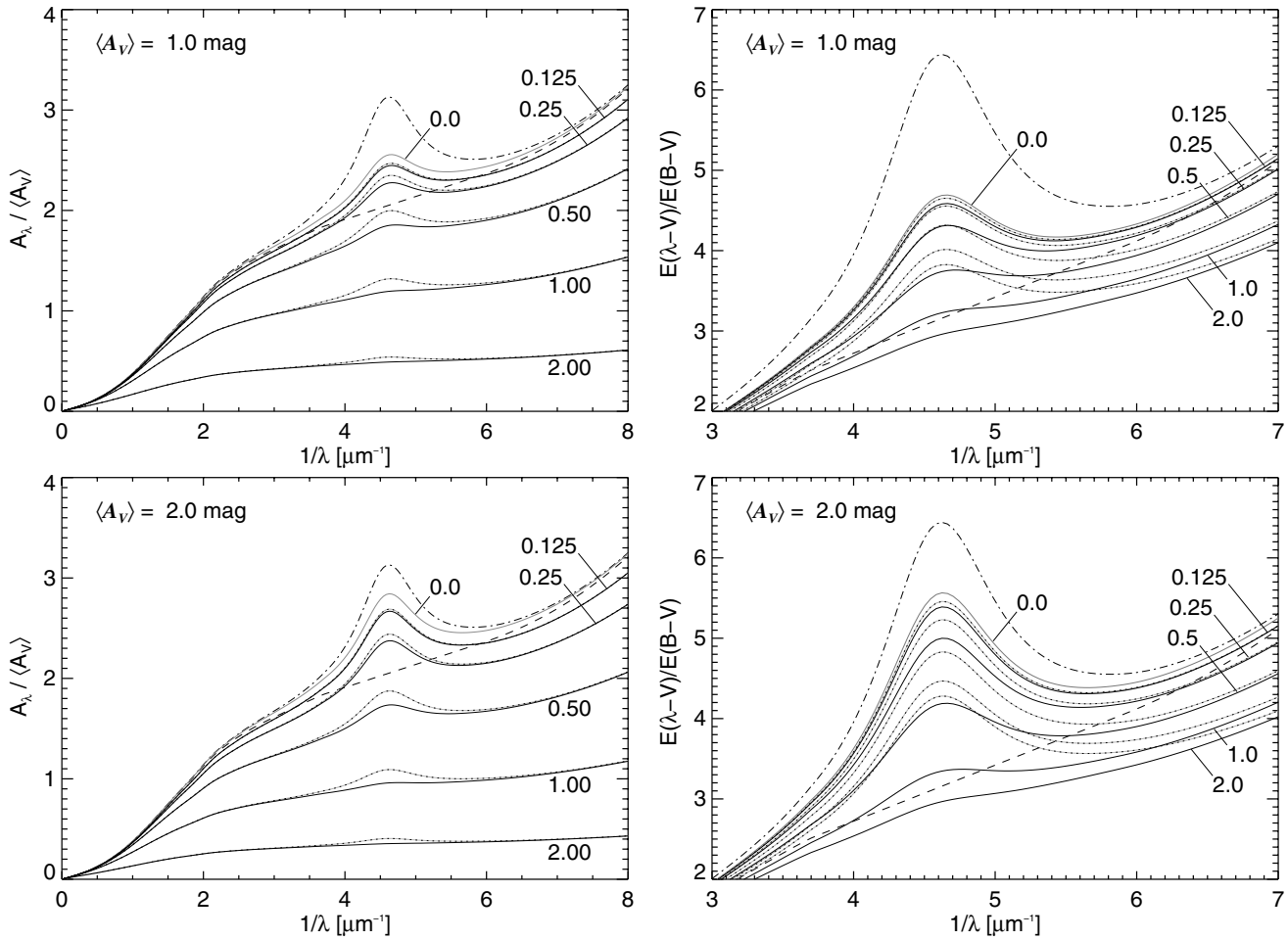

Fig. 2. Effective Extinction curves (*left hand figure*) and reddening curves around the extinction bump (*right hand figure*) for a turbulent distant screen. The intrinsic extinction curves with and without extinction bump are shown as dashed-dotted and as dashed curve, respectively. The effective extinction and reddening curves without and with change of the dust properties as function of optical depth are shown either as dotted curve or solid curves. Added is also the mean extinction curve for the limit of a non turbulent screen (grey curve). It is assumed that the extinction bump at 2175 Å is absent below a column density $N_{\rm H} = 10^{21}$ cm^{-2} which corresponds, assuming $R_V = 3.1$ (Fitzpatrick 1999) and a dust-to-gas-ratio of $N_{\rm H}/E(B-V) = 5.8 \times 10^{21}$ cm^{-2} (Bohlin et al. 1978), to $A_V \approx 0.53$ mag. The curves are labelled with the corresponding standard deviation $\sigma_{\ln\xi}$ of the log-normal density distribution of the normalized column density $\xi = N_{\rm H}/\langle N_{\rm H}\rangle$.

Table 1. Parameters of the attenuation curve.

		$\langle A_V\rangle = 1$ mag			$\langle A_V\rangle = 2$ mag		
$\sigma_{\ln\xi}$	$\sigma_{\rho/\langle\rho\rangle}{}^a$	R_V^A	$\frac{A_V}{\langle A_V\rangle}$	c_3/γ^2	R_V^A	$\frac{A_V}{\langle A_V\rangle}$	c_3/γ^2
0.125	0.28	3.13	0.993	1.44	3.15	0.986	2.27
0.250	0.57	3.21	0.972	1.21	3.31	0.947	1.94
0.500	1.19	3.51	0.896	0.74	3.79	0.825	1.26
1.000	2.93	4.29	0.682	0.37	4.79	0.565	0.54
2.000	16.4	5.54	0.320	0.19	6.11	0.239	0.23

Notes. [(a)] Density contrast based on Eq. (3) assuming $n = -10/3$ and $\Delta/L_{\rm max} = 1$.

3.2. Peak strength

We have analyzed the effect of the additional destruction of a turbulent distant screen on the absorption feature by considering the effective peak strength $\Delta A_{0.22}^{\rm eff}/E(B-V)^{\rm eff}$ where $\Delta A_{0.22}^{\rm eff}$ is the difference of the effective extinction at peak frequency of the complete model and a model where the bump has been removed from the intrinsic extinction curve. To understand the importance of additional destruction we also considered a screen where no further destruction has occurred.

3.2.1. No additional destruction

As found in Paper III the effective extinction curves of the turbulent screen are well determined by the effective absolute-to-relative extinction R_V. For given R_V-value we therefore expect a certain strength of the peak. As Fig. 3 shows, in case of probability distribution functions (PDFs) of the column densities with $\sigma_{\ln\xi} \ll 1$ this behavior is quite accurate. For wide PDFs and high extinction values the R_V-value only provides an approximation of the correct attenuation curves. For example, if we consider a certain R_V-value the peak strength increases for broader PDFs. But still, for $\sigma_{\ln\xi} < 2$ the effect is in the order of only a few percent.

Turbulence not only flattens the extinction curve but also reduces the peak strength as we have seen in the former section. The effects are stronger in more optically thick media but, as Fig. 3 shows, do not simply increase towards wider PDFs of the column density. This behavior is only true for media which are optically thin and for optically thick media with not

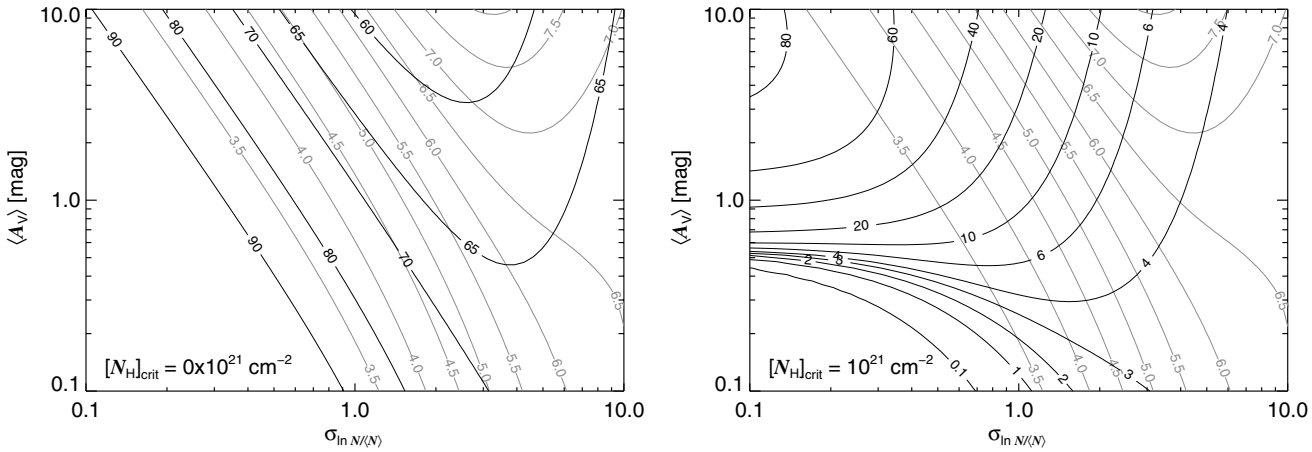

Fig. 3. Peak strength $\Delta A_{0.22}^{\rm eff}/E(B-V)^{\rm eff}$ of the effective extinction curve without (*left*) and with additional destruction (*right*) of the carriers as function of the two parameters $\langle A_V\rangle$ and $\sigma_{\ln N/\langle N\rangle}$ of the turbulent screen. The black curves are lines of constant peak strengths. They are labelled with the percentage of the peak strength relative to the intrinsic value. In *the right figure* the carriers are assumed to be destroyed below a critical column density of $[N_{\rm H}]_{\rm crit} = 10^{21}$ cm^{-2}. The corresponding R_V-values are shown as grey solid lines.

extremely wide PDFs. As shown in Appendix A.2 in the limit of infinitely broad PDFs the R_V-value and the peak strength of the effective extinction curve become independent on the mean extinction $\langle A_V\rangle$ and the standard deviation of the column density $\sigma_{\ln\xi}$. The asymptotic absolute-to-relative extinction is given by $R_V^{\rm eff} = \sqrt{R_V}/(\sqrt{R_V+1}-\sqrt{R_V})$. For $R_V = 3.1$ we have $R_V^{\rm eff} \approx 6.67$. Likewise, we have a limit of the peak strength given by 68%. For media which are optically thick the asymptotic value does not provide the strongest effect on the flatness and peaks strength. But still, for the considered parameter range the peak strength is quite strong with >50%. Turbulence alone is therefore not able to produce the low peak strength of the Calzetti curve.

3.2.2. Additional destruction

As a special example to analyze the effect caused by the additional destruction of the carriers of the peak on its strength we considered again a critical column density of $[N_{\rm H}]_{\rm crit} = 10^{21}$ cm^{-2}. Figure 3 shows a strong reduction of the peak strength even for less broad PDFs. For mean column densities well above the critical column densities the peak strength weakens strongly in case of more turbulent media. For $\langle A_V\rangle < 10$ mag and $\sigma_{\ln\xi} > 2$ the peak strength is lower than 10% relative to the intrinsic value. The impact of the destruction on the carriers weakens for higher extinction values $\langle A_V\rangle$.

In case of turbulent screens with mean column densities well below the critical column density turbulence produces regions of high column densities where the carriers of the peak can survive. As the mass is compressed to more opaque clouds in higher turbulent media the peak strength increases with $\sigma_{\ln\xi}$.

For intermediate mean column densities turbulence leads to an increase at low $\sigma_{\ln\xi}$ but to a decrease of the peak strength at high $\sigma_{\ln\xi}$.

In the limit of broad PDFs of the column density the peak strength reaches asymptotically a value which is independent on the main parameters of the screen, the mean extinction $\langle A_V\rangle$ and standard deviation of the log-normal function $\sigma_{\ln\xi}$. It solely depends on the critical column density $[N_{\rm H}]_{\rm crit}$ and allows therefore a first estimate of the possible effect caused by the additional destruction on the peak strength. The asymptotic behavior is analyzed in Appendix A.2. For the critical column density assumed in Fig. 3 the asymptotic value is 3.3% of the intrinsic peak strength. As shown in Appendix A.2 for larger critical column densities the asymptotic value of the peak strength decreases strongly as $\tau_1^{-3/2}\,{\rm e}^{-\tau_1}$ where $\tau_1 = \kappa_{0.22}^{(1)}[N_{\rm H}]_{\rm crit}$. For critical column densities well below $[N_{\rm H}]_{\rm crit} = 10^{21}$ cm^{-2} the asymptotic peak strength reaches the value of 68% caused by the turbulence in the limit of broad PDFs as discussed above.

The effect of the critical column density on the peak strength is more accurately derived in Fig. 4. The figure shows the critical column density needed to reduce the peak strength to 10% and 50% of the intrinsic value. To produce a peak strength of turbulent screens with $\sigma_{\ln\xi} > 1$ and $\langle A_V\rangle < 10$ mag by more than 50% the critical column density needs to be at least $\sim 3\times 10^{20}$ cm^{-2}. To decrease in the same parameter range of the screen the peak strength to 10% of its intrinsic value the critical column density needs to be at least $\sim 2\times 10^{21}$ cm^{-2}. As the figure shows the critical column density cannot be considerably smaller than 10^{21} cm^{-2} to produce peak strengths as low as 10%. For example, a critical column density of 6×10^{21} cm^{-2} would require in case of screens ($\langle A_V\rangle > 1$ mag) very broad PDFs with $\sigma_{\ln\xi} > 4$ which would imply Mach numbers $M > 1500$ far above the ones measured in the ISM of our galaxy.

4. Conclusion

The analysis shows that a turbulent distant screen can naturally explain not only the flatter curvature but also a weak absorption feature at 2175 Å of the Calzetti-curve if within a certain column density its carriers are destroyed by the strong UV-radiation in star-burst galaxies. The feature is efficiently reduced by more than 80% of its intrinsic value if the following circumstances are fulfilled for typical extinction values measured for star burst galaxies ($A_V \sim 1$ mag):

- The standard deviation of the log-normal distribution must be larger than $\sigma_{\ln\xi} = 1$.
- The critical column density needs to be larger than $[N_{\rm H}]_{\rm crit} > 10^{21}$ cm^{-2}.

The condition for the standard deviation of the log-normal distribution of the column density is in agreement with the Mach number of the cold neutral medium (which implies $\sigma_{\rho/\langle\rho\rangle} \sim 6$) if the

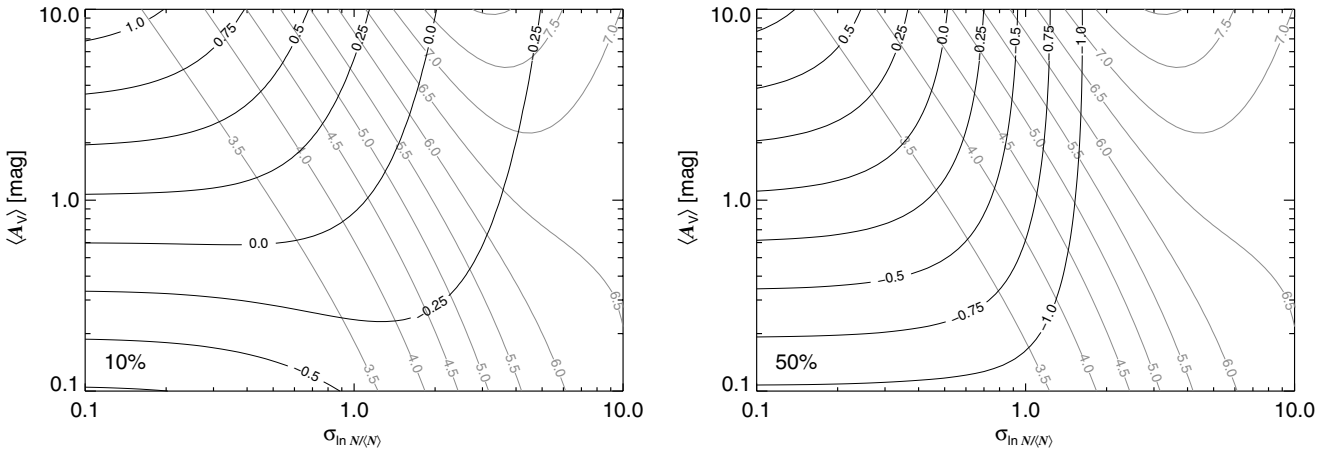

Fig. 4. Critical column density $[N_{\rm H}]_{\rm crit}$ needed to reduce the peak strength $\Delta A_{0.22}^{\rm eff}/E(B-V)^{\rm eff}$ of the effective attenuation curve of a turbulent screen to 10% (*left hand figure*) or 50% (*right hand figure*) of the intrinsic value. The curves are labelled by $\log N_{\rm H}[10^{21}\ {\rm cm}^{-2}]$. The grey curves give the effective R_V-value.

thickness is not sufficiently larger than a few turbulent length scales.

A fractal density structure can also enhance the probability for the carriers' survival as they become located in optical thick clouds and therefore save against further destruction by a strong UV-field.

Acknowledgements. Dopita & Fischera acknowledge financial support under Discovery project DP0984657.

Appendix A: Approximation

If we consider an optically thick medium then turbulence will lead to regions of low column density through which most of the light will be transmitted. The effective attenuation curve is determined by those regions. If the medium becomes on the other hand highly turbulent the medium is compressed to very small clouds. The only attenuation occurs in regions of high column density which determine the attenuation curve. To differentiate the two different cases we can consider the column density $N_{\rm H} = \langle N_{\rm H}\rangle {\rm e}^{y}$ where $\tau = 1$ relative to the column density at maximum position of the log-normal distribution $N_{\rm H} = \langle N_{\rm H}\rangle {\rm e}^{-0.5\sigma^2_{\ln\xi}}$. We distinguish the cases $-\ln\langle\tau\rangle \ll -0.5\sigma^2_{\ln\xi}$ and $-\ln\langle\tau\rangle \gg -0.5\sigma^2_{\ln\xi}$

A.1. Approximation for $ln\langle\tau\rangle \gg 0.5\sigma^2_{ln\xi}$

The deviation of the approximation for $\ln\langle\tau\rangle \gg 0.5\sigma^2_{\ln\xi}$ follows the procedure presented in Paper III. For sake of simplicity we ignore the additional dependence on wavelength. In this limit the integrands of Eq. (5) become narrow functions around the maxima at $\tilde{y}_i$ determined by

$$f'(\tilde{y}_i) = -\langle\tau_i\rangle {\rm e}^{\tilde{y}_i} - \frac{1}{\sigma^2}\left(\tilde{y}_i + \frac{1}{2}\sigma^2_{\ln\xi}\right) = 0 \tag{A.1}$$

where $\tilde{y}_1$ is the location of the maximum of the first and $\tilde{y}_2$ the location of the maximum of the second integrand. Developing the exponential function in the exponent around these maxima to a secondary order polynomial funtion

$${\rm e}^{y} \approx {\rm e}^{\tilde{y}_i}(1 + (y-\tilde{y}_i) + \frac{1}{2}(y-\tilde{y}_i)^2) \tag{A.2}$$

for $i = 1, 2$ leads to the approximate expression of the effective extinction

$${\rm e}^{-\tau^{\rm eff}} = {\rm e}^{-\tau_1^{\rm eff}}\frac{1+erf(t_1)}{2} + {\rm e}^{-\tau_2^{\rm eff}}\frac{1-erf(t_2)}{2}. \tag{A.3}$$

where

$$erf(t_i) = \frac{2}{\sqrt{\pi}}\int_0^{t_i} {\rm d}y\, {\rm e}^{-y^2} \tag{A.4}$$

is the error function and where

$$t_i = \sqrt{\frac{\gamma_i}{2\sigma^2_{\ln\xi}}}(y_{\rm crit} - \tilde{y}_i), \quad \gamma_i = 1 + \langle\tau_i\rangle\sigma^2_{\ln\xi}{\rm e}^{\tilde{y}_i}. \tag{A.5}$$

The effective optical depths are given by:

$$\tau_1^{\rm eff} = \frac{1}{2}\ln\gamma_1 + \frac{1}{2}\langle\tau_1\rangle{\rm e}^{\tilde{y}_1}(1+\gamma_1), \tag{A.6}$$

$$\tau_2^{\rm eff} = \frac{1}{2}\ln\gamma_2 + \Delta\langle\tau\rangle{\rm e}^{y_{\rm crit}} + \frac{1}{2}\langle\tau_2\rangle{\rm e}^{\tilde{y}_2}(1+\gamma_2). \tag{A.7}$$

In Paper III we have shown that the approximation provides the correct results also for small fluctuations $\sigma_{\ln\xi} \ll 1$ for all optical depths. In the limit of small fluctuations we obtain the natural optical depths of a homogeneous screen as $\gamma_i \to 1$ and $\tilde{y}_i \to 0$.

Figure A.1 shows peak strengths derived using the approximation. They are compared with accurate calculations. The approximation becomes more accurate for smaller standard deviations and larger extinction values. For optical thick media ($\langle A_V\rangle > 1$ mag) the approximation is accurate for $\sigma_{\ln\xi} \le 1$.

The approximation can be used to estimate if the effective extinction curve is either a flat curve, so that $\tau_\lambda^{\rm eff} \approx \tau_\lambda^{\rm eff,1}$, or "peak dominated", so that $\tau_\lambda^{\rm eff} \approx \tau_\lambda^{\rm eff,2}$. The effective extinction is "peak dominated" if the critical value lies well below the typical column densities contributing to the effective extinction ${\rm e}^{-\tau^{\rm eff,2}}$. As a simple criterium we can consider $t_i = 0$ for $i = 1, 2$ which provides for given mean and critical column density a critical standard deviation

$$\sigma^{\rm crit,i}_{\ln\xi} = \sqrt{\frac{-2y_{\rm crit}}{2\kappa^{(i)}_{0.22\ \mu{\rm m}}[N_{\rm H}]_{\rm crit}+1}}, \quad y_{\rm crit} \le 0. \tag{A.8}$$

where $\kappa^{(i)}_{0.22\ \mu{\rm m}}$ are the extinction coefficients given in Eq. (6).

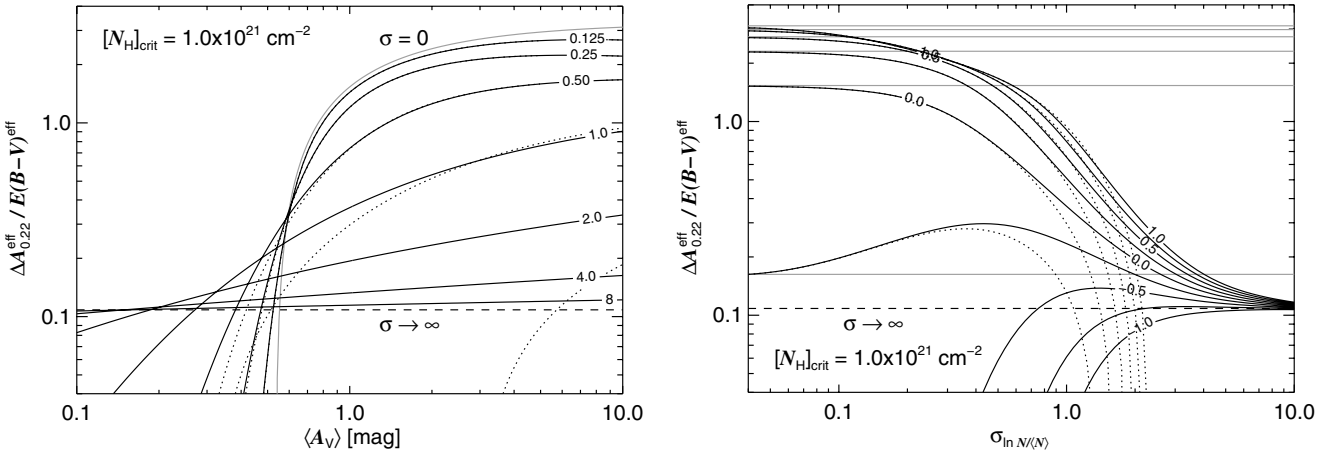

Fig. A.1. Peak strength of the effective extinction curve caused by a distant turbulent screen as function of the mean extinction ($\langle A_V \rangle$) for given column density contrast ($\sigma_{lnN/\langle N\rangle}$) (*left hand figure*) and as function of column density contrast for given mean extinction (*right hand figure*). The curves in *the right hand figure* are labelled with $\log A_V$[mag]. The critical column density is assumed to be $[N_{\rm H}]_{\rm crit} = 10^{21}$ cm^{-2}. The values in the limit of a non turbulent medium ($\sigma = 0$) are shown as grey lines, the value in the the theoretical limit of infinite column density contrast ($\sigma \to \infty$) as dashed line. Also shown as dotted lines are peak strengths derived using the approximation Eq. (A.3).

Table A.1. Critical standard deviations.

$\langle A_V \rangle$	[mag]	1.00	2.00	1.00	2.00
$[N_{\rm H}]_{\rm crit}$	[10^{21} cm^2]	0.50	0.50	1.00	1.00
$\sigma^{\rm crit,1}_{\ln\xi}$		1.15	1.42	0.65	0.94
$\sigma^{\rm crit,2}_{\ln\xi}$		1.02	1.27	0.56	0.81

The extinction curve is "peak dominated" for $t_2 \ll 0$ ($\sigma_{\ln\xi} \ll \sigma^{\rm crit,2}_{\ln\xi}$) as the error functions become $erf(t_1) = erf(t_2) = -1$. In the additional limit $[N_{\rm H}]_{\rm crit}/\langle N_{\rm H}\rangle \ll 1$ we obtain the result of Paper III

$$\tau^{\rm eff,2}_\lambda = \frac{1}{2}\ln\gamma_2 + \frac{1}{2}\langle\tau^2\rangle e^{\tilde{y}_2}(1+\gamma_2). \quad (A.9)$$

This solution is trivial for $\kappa^{(1)}_\lambda = \kappa^{(2)}_\lambda$ as $t_1 = t_2$. The effective extinction becomes essentially flat for $t_1 \gg 0$ ($\sigma_{\ln\xi} \gg \sigma^{\rm crit,1}_{\ln\xi}$). A number of critical standard deviations are listed for given mean extinction and critical column density in Table A.1. The values point to a critical column density $[N_{\rm H}]_{\rm crit} \geq 10^{21}$ cm^{-2} to obtain a flat extinction curve as lower values would imply wider PDFs which become unlikely considering the density contrast in the ISM of our Galaxy.

A.2. Approximation for $ln\langle\tau\rangle \ll 0.5\sigma^2_{ln\xi}$

In the limit $-\ln\langle\tau\rangle \gg -0.5\sigma^2_{\ln\xi}$ most sight lines through the turbulent medium are optically thin. It is therefore convenient to rewrite the equation for the effective optical depth so that

$$\tau^{\rm eff}_\lambda = -\ln\left\{1 - \int {\rm d}y\, p(y)\left(1 - e^{-\langle\tau\rangle e^y}\right)\right\}. \quad (A.10)$$

The integral is a small number so that

$$\tau^{\rm eff}_\lambda \approx \int {\rm d}y\, p(y)\left(1 - e^{-\langle\tau\rangle e^y}\right). \quad (A.11)$$

In case that $y \ll 0.5\sigma^2$ we can replace the PDF of the column density through a power law distribution:

$${\rm d}y\, p(y) \approx {\rm d}\tau \frac{e^{-\sigma^2/8}}{\sqrt{2\pi}\sigma}\frac{\sqrt{\langle\tau\rangle}}{\sqrt[3]{\tau}} \quad (A.12)$$

where $\tau = \langle\tau\rangle \ln y = \kappa[N_{\rm H}]_{\rm crit}$. The equation for the effective optical depth becomes after an additional partial integration:

$$\tau^{\rm eff} \approx \sqrt{\frac{2}{\pi}}\frac{e^{-\sigma^2/8}}{\sigma}\sqrt{\langle\tau\rangle}\int_0^\infty {\rm d}t\, t^{-1/2}\, e^{-t} \quad (A.13)$$

where the integral can be identified as the Γ-function with $\Gamma(\frac{1}{2}) = \sqrt{\pi}$.

In the limit of a broad PDF the effective optical depth decreases strongly with $\sigma_{\ln\xi}$ and is proportional to the square root of the mean optical depth. The ratio of two effective optical depths becomes not only independent on the width of the PDF but also independent on the dust content of the screen. As a special case we can consider the absolute to relative extinction value $R_V = A_V/(A_B - A_V)$. The corresponding value of a turbulent screen with an infinite broad PDF has then a value of $1/R^{\rm eff}_V = \sqrt{1 + R_V^{-1}} - 1$. For $R_V = 3.1$ we obtain therefore an asymptote $R^{\rm eff}_V \approx 6.67$. Another example is the peak strength. If we ignore additional destruction the peak strength in case of broad PDFs of the column density approaches asymptotically

$$\frac{\Delta A^{\rm eff}}{E(B-V)^{\rm eff}} = \frac{\sqrt{\kappa^{(2)}_{0.22}} - \sqrt{\kappa^{(1)}_{0.22}}}{\sqrt{\kappa_B} - \sqrt{\kappa_V}} = 2.23. \quad (A.14)$$

Compared to the intrinsic value of 3.30 this means a reduction to 68% in the limit of infinite broad PDFs.

A similar approach leads to the asymptotic behavior of the peak strength in case of additional destruction. The equation for the effective optical depth at peak frequency can be rewritten as:

$$\begin{aligned}\tau^{\rm eff} = -\ln\Big\{1 &- \int_{y_{\rm crit}}^\infty {\rm d}y\, p(y)\left(1 - e^{-\Delta\langle\tau\rangle_{\rm crit}}\right) \\ &- \int_{-\infty}^\infty {\rm d}y\, p(y)\left(1 - e^{-\langle\tau_1\rangle e^y}\right) + \int_{y_{\rm crit}}^\infty {\rm d}y\, p(y)\left(1 - e^{-\langle\tau_1\rangle e^y}\right) \\ &- e^{-\Delta\langle\tau\rangle_{\rm crit}}\int_{y_{\rm crit}}^\infty {\rm d}\, p(y)\left(1 - e^{-\langle\tau_2\rangle e^y}\right)\Big\}. \quad (A.15)\end{aligned}$$

The sum over the four integrals is a small number so that we can make the same simplification as in Eq. (A.11). Replacing the

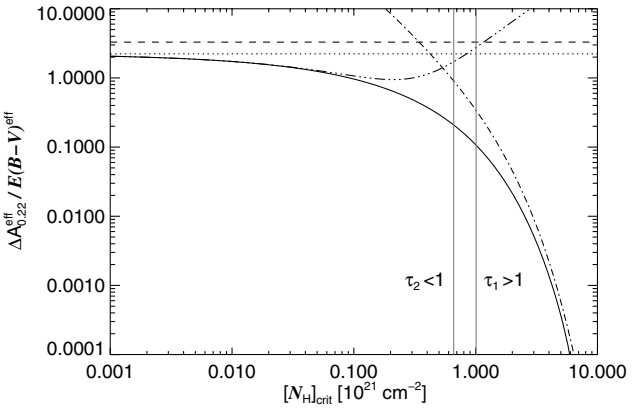

Fig. A.2. Peak strength in the limit of a broad PDF with $\ln\langle\tau\rangle \ll \frac{1}{2}\sigma^2_{\ln\xi}$ as function of the critical column density below which the carriers of the peak are assumed to be destroyed. The intrinsic peak strength as given by Fitzpatrick (1999) is shown as dashed line. The corresponding peak strength of a turbulent screen model with no additional destruction is shown as dotted line. The dashed-dotted and the three dashed-dotted curves are the approximations in the regime $\tau_1 = \kappa^{(1)}_{0.22}[N_{\rm H}]_{\rm crit} \gg 1$ and $\tau_2 = \kappa^{(2)}_{0.22}[N_{\rm H}]_{\rm crit} \ll 1$ given in Eqs. (A.21) and (A.23).

distribution of the column density by the power law distribution (Eq. (A.12)) provides:

$$\tau^{\rm eff} \approx \sqrt{\frac{2}{\pi}}\frac{{\rm e}^{-\sigma^2/8}}{\sigma}\Big\{\sqrt{\langle N_{\rm H}\rangle/[N_{\rm H}]_{\rm crit}}\left(1-{\rm e}^{-\Delta\langle\tau\rangle_{\rm crit}}\right) + \sqrt{\langle\tau_1\rangle}\,(f(0)-f(\tau_1)) + \sqrt{\langle\tau_2\rangle}\,f(\tau_2)\,{\rm e}^{-\Delta\langle\tau\rangle_{\rm crit}}\Big\}, \quad (A.16)$$

where

$$f(\tau) = \frac{1}{2}\int_\tau^\infty {\rm d}t\, t^{-3/2}\left(1-{\rm e}^{-t}\right) = \frac{1-{\rm e}^{-\tau}}{\sqrt{\tau}} + \Gamma\left(\frac{1}{2},\tau\right). \quad (A.17)$$

$\Gamma(a,x)$ is the incomplete Γ-function

$$\Gamma(a,x) = \int_x^\infty {\rm d}t\, t^{a-1}{\rm e}^{-t}. \quad (A.18)$$

For the special case $\tau = 0$ we have $f(0) = \sqrt{\pi}$.

For the peak strength in the limit of an infinite broad PDF we obtain:

$$\frac{\Delta A_{0.22}^{\rm eff}}{E(B-V)^{\rm eff}} = \frac{1}{\sqrt{\pi}\sqrt{\kappa_B}-\sqrt{\pi}\sqrt{\kappa_V}}\times\left\{\frac{1}{\sqrt{[N_{\rm H}]_{\rm crit}}}(1-{\rm e}^{-\Delta\tau_{\rm crit}}) + \sqrt{\kappa_2}\,f(\tau_2)\,{\rm e}^{-\Delta\tau_{\rm crit}} - \sqrt{\kappa_1}\,f(\tau_1)\right\}. \quad (A.19)$$

The curve is shown in Fig. A.2. For $[N_{\rm H}]_{\rm crit} \ll 10^{21}$ cm^{-2} the asymptotic value becomes equal to the peak strength with no further destruction. The asymptotic value for $[N_{\rm H}]_{\rm crit} = 10^{21}$ cm^{-2} is added in Fig. A.1. In the limit $y_{\rm crit} \gg -\ln\langle\tau_1\rangle$ we can replace the incomplete Gamma function by

$$\int_x^\infty t^{a-1}\,{\rm e}^{-t} \approx x^{s-1}{\rm e}^{-x}\left(1+(s-1)x^{-1}\right) \quad (A.20)$$

which leads to

$$\Delta\tau^{\rm eff} \approx \sqrt{\frac{2}{\pi}}\frac{{\rm e}^{-\sigma^2/8}}{\sigma}\times\sqrt{\frac{\langle N_{\rm H}\rangle}{[N_{\rm H}]_{\rm crit}}}\frac{1}{2}\left(\frac{1}{\tau_1}-\frac{1}{\tau_2}\right){\rm e}^{-\tau_1}. \quad (A.21)$$

At $[N_{\rm H}]_{\rm crit} \gg 10^{21}$ cm^{-2} the asymptotic peak strength decreases as $\tau_1^{-3/2}{\rm e}^{-\tau_1}$.

In the limit $y_{\rm crit} \ll -\ln\langle\tau_2\rangle$ we can use the approximation

$$f(\tau) \approx \sqrt{\pi} - \sqrt{\tau} \quad (A.22)$$

which provides:

$$\Delta\tau^{\rm eff} \approx \sqrt{\frac{2}{\pi}}\frac{{\rm e}^{-\sigma^2/8}}{\sigma}\Big\{\sqrt{\langle\tau_2\rangle}\left[\sqrt{\pi}(1-(\tau_1-\tau_2)) - 2\sqrt{\tau_2}\right] - \sqrt{\langle\tau_1\rangle}\left(\sqrt{\pi}-2\sqrt{\tau_1}\right)\Big\}. \quad (A.23)$$

This approximation provides accurate asymptotic peak strength below $[N_{\rm H}]_{\rm crit} = 10^{20}$ cm^{-2}.

References

Allain, T., Leach, S., & Sedlmayr, E. 1996a, A&A, 305, 602
Allain, T., Leach, S., & Sedlmayr, E. 1996b, A&A, 305, 616
Allamandola, L. J., Tielens, A. G. G. M., & Barker, J. R. 1989, ApJS, 71, 733
Bohlin, R. C., Savage, B. D., & Drake, J. F. 1978, ApJ, 224, 132
Calzetti, D. 2001, PASP, 113, 1449
Calzetti, D., Bohlin, R. C., Gordon, K. D., Witt, A. N., & Bianchi, L. 1995, ApJ, 446, L97
Dopita, M., Groves, B., Fischera, J., et al. 2005, ApJ, 619, 755
Draine, B. T., & Li, A. 2007, ApJ, 657, 810
Fischera, J., & Dopita, M. 2004, ApJ, 611, 911
Fischera, J., & Dopita, M. 2005, ApJ, 619, 340
Fischera, J., & Dopita, M. 2008, ApJS, 176, 164
Fischera, J., Dopita, M., & Sutherland, R. 2003, ApJ, 599, L21
Fitzpatrick, E. L. 1999, PASP, 111, 63
Gordon, K. D., & Clayton, G. C. 1998, ApJ, 500, 816
Gordon, K. D., Calzetti, D., & Witt, A. N. 1997, ApJ, 487, 625
Gordon, K. D., Clayton, G. C., Misselt, K. A., Landolt, A. U., & Wolff, M. J. 2003, ApJ, 594, 279
Granato, G. L., Lacey, C. G., Silva, L., et al. 2000, ApJ, 542, 710
Le Page, V., Snow, T. P., & Bierbaum, V. M. 2003, ApJ, 584, 316
Léger, A., D'Hendecourt, L., Boissel, P., & Desert, F. X. 1989, A&A, 213, 351
Lequeux, J., Maurice, E., Prevot-Burnichon, M., Prevot, L., & Rocca-Volmerange, B. 1982, A&A, 113, L15
Li, A., & Draine, B. T. 2001, ApJ, 554, 778
Lillie, C. F., & Witt, A. N. 1976, ApJ, 208, 64
Morgan, D. H., Nandy, K., & Thompson, G. I. 1976, MNRAS, 177, 531
Omont, A. 1986, A&A, 164, 159
Padoan, P., Jones, B., & Nordlund, k. 1997, ApJ, 474, 730
Panuzzo, P., Granato, G. L., Buat, V., et al. 2007, MNRAS, 375, 640
Russell, S. C., & Dopita, M. A. 1992, ApJ, 384, 508
Weingartner, J. C., & Draine, B. T. 2001, ApJ, 548, 296
Witt, A. N., & Gordon, K. D. 2000, ApJ, 528, 799
Witt, A. N., & Lillie, C. F. 1973, A&A, 25, 397
Witt, A. N., Walker, G. A. H., Bohlin, R. C., & Stecher, T. P. 1982, ApJ, 261, 492
Witt, A. N., Petersohn, J. K., Bohlin, R. C., et al. 1992, ApJ, 395, L5